

1-1-2021

A new dataset for smartphone gesture-based authentication

Eliu Huang
San Jose State University

Fabio Di Troia
San Jose State University, fabio.ditroia@sjsu.edu

Mark Stamp
San Jose State University, mark.stamp@sjsu.edu

Preethi Sundaravaradhan
San Jose State University

Follow this and additional works at: https://scholarworks.sjsu.edu/faculty_rsca

Recommended Citation

Eliu Huang, Fabio Di Troia, Mark Stamp, and Preethi Sundaravaradhan. "A new dataset for smartphone gesture-based authentication" *ICISSP 2021 - Proceedings of the 7th International Conference on Information Systems Security and Privacy* (2021): 771-780. <https://doi.org/10.5220/0010425807710780>

This Conference Proceeding is brought to you for free and open access by SJSU ScholarWorks. It has been accepted for inclusion in Faculty Research, Scholarly, and Creative Activity by an authorized administrator of SJSU ScholarWorks. For more information, please contact scholarworks@sjsu.edu.

A New Dataset for Smartphone Gesture-based Authentication

Elliu Huang^a, Fabio Di Troia^b, Mark Stamp^c and Preethi Sundaravaradhan^d

Department of Computer Science, San Jose State University, San Jose, California, U.S.A.

Keywords: Gesture, Authentication, Accelerometer, Support Vector Machine, Principal Component Analysis.

Abstract: In this paper, we consider the problem of authentication on a smartphone, based on gestures. Specifically, the gestures consist of users holding a smartphone while writing their initials in the air. Accelerometer data from 80 subjects was collected and we provide a preliminary analysis of this data using machine learning techniques. The machine learning techniques considered include principal component analysis (PCA) and support vector machines (SVM). The results presented here are intended to provide a baseline for additional research based on our dataset.

1 INTRODUCTION

Authentication is an integral part of the security of any digital system. Several methods of authentication are available, with passwords being the most common. Another popular form of authentication relies on biometric features of users. As with any authentication technique, a useful biometric must enable us to distinguish between users and, to be practical, such features must be easy to collect in a reliable manner.

Biometric authentication can be divided into two categories based on whether the users are identified by their physical features or their behavioral patterns (Ganesh et al., 2017). A new type of behavioral biometric authentication system inspired by handwritten signatures has recently been considered (Yang et al., 2015). This system involves signing gestures in the air, similar to drawing signatures with a pen.

One such system is OpenSesame, which is claims to achieve a high-level of security and robustness, with a mean false positive rate of 15% and a false negative rate of 8% (Yang et al., 2015). OpenSesame evaluates hand gesture actions, but does not take into account a “shoulder surfing” scenario, that is, the case where an intruder observes a user’s hand movements and then imitates the movements in an attempt to gain access to the system. This scenario is analogous to forging a signature on paper.

Several machine learning techniques have been

used to recognize gesture-based signatures in the form of accelerometer sensor data. Among the most popular machine learning techniques for this purpose are hidden Markov models (HMM) (Bailador et al., 2011; Rabiner, 1989), support vector machines (SVM), recurrent neural networks (RNN), and dynamic time warping (DTW) (Mitra and Acharya, 2007; Yang et al., 2015).

In this research, we explore the effectiveness and robustness of gesture-based authentication, based on a new and substantial dataset that we have collected. Specifically, we consider the accuracy that can be achieved using accelerometer data based on in-air handwriting, and we also consider the effectiveness of shoulder surfing attacks on such a system. We measure effectiveness in terms of the accuracy of user identification and intruder detection.

To analyze our accelerometer data, we consider machine learning strategies. We focus on SVMs and we also experiment with PCA for dimensionality reduction. Research in gesture-based authentication systems often focuses on detecting the shape and stroke of the pattern (Huang et al., 2017). In this paper, we consider statistical features, without explicitly identifying the shape of the signature.

The remainder of this paper is organized as follows. Section 2 provides relevant background on a variety of topics, including related authentication systems, machine learning techniques, and data collection. In Section 3, we discuss our data collection process, and we provide details on our experiments and results. Section 4 gives our conclusions along with suggestions for future work.

^a <https://orcid.org/0000-0001-7515-7369>

^b <https://orcid.org/0000-0003-2355-7146>

^c <https://orcid.org/0000-0002-3803-8368>

^d <https://orcid.org/0000-0002-0966-0852>

2 BACKGROUND

In this section, we first introduce the problem under consideration and briefly discuss relevant previous work. Then we mention the metrics used to measure the success of our experiments and we also briefly introduce the machine learning techniques that we employ. Data collection and feature extraction are a major emphasis of this work, so we discuss these issues in more detail.

2.1 Motivation

A machine can authenticate a user by means of something the user knows (typically, a password), or something the user possesses (e.g., an RFID tag), or by some characteristic of the user (e.g., a biometric feature such as a fingerprint). These are popularly summarized in the security domain as “something you know, something you have, or something you are” (Anderson, 2001). This research is focused on a biometric authentication technique based on smartphone movements, as measured by a built-in accelerometer.

There are two broad categories of biometrics—physical based and behavioral based. Physical based biometrics verify a user based on an innate characteristic, such as an iris scan, fingerprint, hand geometry, or facial recognition. Such authentication involves scanning the biometric feature of the user and attempting to matching the result to a stored version that is assumed to belong to the specified user.

Behavioral biometrics, which are also known as physiological biometrics, verify a user based on some specific behavior (Huang et al., 2017). Features used in such an authentication technique depend on knowledge of a user’s behavior. For example, an image of a handwritten signature can be captured and image-based pattern recognition can then be used for authentication (Bailador et al., 2011). Another example of a behavior based biometric is keystroke dynamics (Liu et al., 2009a), where, for example, a time-series analysis can be applied to timing data that is recorded while typing. Gait recognition is yet another behavioral based biometric—such systems leverage the speed and motion pattern of users, based on video or audio signals (Huang et al., 2018; Liu et al., 2017).

There are a wide variety of attacks on authentication systems in general. For example, in the case of password based authentication, an attacker might steal a password file containing hashed passwords and conduct a forward search attack (Stamp, 2011). In the case of biometric authentication, attacks typically involve copying the biometric features (Guse, 2011a).

A gesture-based authentication scheme might offer some resistance to such attacks, in part due to the fact that the search space for relevant patterns is potentially very large (Bailador et al., 2011). In addition to knowing the pattern itself, the attacker might need to know something about the angle, speed, and relative area in which the pattern is drawn (Guse, 2011a).

The authentication technique considered in this paper, which is based on gestures captured using an accelerometer sensor, can be categorized as a behavioral biometric. A similar type of biometric system is considered, for example, in (Huang et al., 2017). Under our approach, 3-d accelerations are captured when the user waves a phone in a manner analogous to writing their own initials. The resulting sensor data is a sequence of (x, y, z) triples that correspond to acceleration in the respective planes. In our experiments, we process these sequences to obtain features that are used by machine learning algorithms for classification. Our goal is to determine how accurately we can distinguish between users, as well as to determine the susceptibility of such an authentication technique to shoulder surfing attacks.

Our gesture-based authentication scheme requires an accelerometer. Fortunately, virtually all modern smart devices have a built-in accelerometer, which makes such sensors nearly ubiquitous. We note in passing that authentication based on accelerometer data is computationally cheaper than facial recognition and many other comparable types of physical biometrics (Huang et al., 2017). Thus, the authentication technique considered here is eminently practical, and may be of particular interest in the case of resource-constrained smart devices.

2.2 Related Work

The two main methods by which gesture-based authentication has been approached are via motion gestures and touchscreen (Clark and Lindqvist, 2014). Approaches using motion gestures generally use accelerometer and gyroscope data, and prior research in this domain have applied DTW (Liu et al., 2009b) and SVMs (Lu et al., 2018). Accelerometer and gyroscope data have also been collected via mobile devices in (Guse, 2011b), which applies DTW and HMMs to authenticate users. A more sophisticated method involves a sensor known as the Leap Motion controller to collect 3-d motion data and applies similarity thresholds to authenticate users (Imura and Hosobe, 2018).

Touchscreen-based gesture authentication methods typically analyze touch dynamics, i.e., various inputs recorded from a touchscreen interface, such as

finger size and pressure. One study analyzed finger behavior and position data, authenticating users using SVMs (Alariki and Manaf, 2014). Another study employed neural networks, specifically particle swarm optimization (PSO), to find patterns in touch dynamics (Meng et al., 2013).

An important component of authentication is forgery, and prior research into gesture authentication forgery can be divided into naive and visual forgery. In naive forgery, attackers randomly guess the pattern because they do not know their target user’s signature, similar to randomly guessing passwords. Visual forgery, also known as shoulder surfing, describes the situation in which attackers imitate another user’s gestures after seeing the user’s signature. A variety of techniques have been applied to combat both naive and visual forgery, such as DTW for the former and HMMs for the latter (Guse, 2011b).

2.3 Metrics

In this section, we discuss the metrics we use to measure the quality of our authentication experiments. Generically, two types of errors can occur in authentication systems. The rate at which an intruder is erroneously recognized as an authentic user is the false acceptance rate (FAR) or, colloquially, the fraud rate. On the other hand, an authentic user may be incorrectly rejected as an intruder—the rate at which this type of mis-authentication occurs is the false reject rate (FRR) or, informally, the insult rate.

A confusion matrix can be used to summarize the following exhaustive and mutually exclusive cases:

True Positive. (TP), where a legitimate user is correctly authenticated as such.

False Positive. (FP), where an intruder is mis-authenticated as a legitimate user.

True Negative. (TN), where an intruder is unable to authenticated as a legitimate user.

False Negative. (FN), where a legitimate user is unable to authenticate as themselves.

Note that TP and TN represent correct classifications, while FP and FN are incorrect classifications and hence the accuracy is given by

$$\text{accuracy} = \frac{TP + TN}{TP + TN + FP + FN}$$

An example of a confusion matrix is illustrated in Figure 1. From such a matrix, the FAR and the FRR are easily computed as

$$\text{FAR} = \text{FPR} = \frac{FP}{FP + TP}$$

and

$$\text{FRR} = \text{FNR} = 1 - \text{TPR} = \frac{TP}{TP + FN}$$

where FPR is the false positive rate, and TPR is the true positive rate.

		Actual Label	
		User A	Intruder
Predicted Label	User A	TP	FP
	Intruder	FN	TN

Figure 1: Confusion matrix.

For a given biometric authentication system, we must set a threshold to distinguish between an authentication success and a failure. This threshold will determine the FAR and FRR. There is an inherent trade-off between the FAR and FRR—changing the threshold to decrease one will necessarily increase the other. The equal error rate (EER) is the rate at which the FAR and FRR are balanced, and can serve as a useful measure for comparing the effectiveness of different biometric systems. A lower equal error rate implies that the system has higher accuracy (Stamp, 2011).

Given a scatterplot of scores, a receiver operating characteristic (ROC) curve provides a graphical illustration of the FPR versus the TPR as the threshold varies through all possible values. The area under the ROC curve (AUC) ranges between 0 and 1, and can be interpreted as the probability that a randomly selected positive instance scores higher than a randomly selected negative instance (Bradley, 1997). If the AUC is $x < 0.5$, we can simply reverse the sense of the classifier to obtain an AUC of $1 - x > 0.5$.

The EER is easily determined from an ROC curve by simply finding the point on the curve where

$$\text{FPR} + \text{TPR} = 1.$$

In the example given in Figure 2, the shaded region representing the AUC, while the point where the main diagonal crosses the ROC curve gives the EER.

2.4 Machine Learning Techniques

A biometric system typically computes a score for a given characteristic by extracting features and then

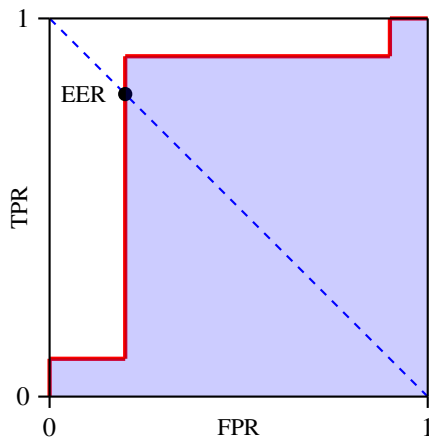


Figure 2: ROC curve and EER.

employs pattern matching or machine learning techniques to determine the classification. In our gesture-based authentication experiments, we employ machine learning algorithms based on features derived from accelerometer data. We employ SVMs as a direct approach and also consider the effect of PCA for dimensionality reduction. Next, we briefly discuss these two machine learning techniques.

2.4.1 Support Vector Machines

Support vector machines (SVMs) are a class of supervised machine learning algorithms that can be used for both regression and classification (Suriya Prakash et al., 2012). With an SVM, we attempt to separate labeled data points by finding an optimal hyperplane, in the sense of maximizing the “margin” or separation between classes. Samples are then classified, depending on which side of the hyperplane they reside. Figure 3 gives an illustrative example of such a hyperplane.

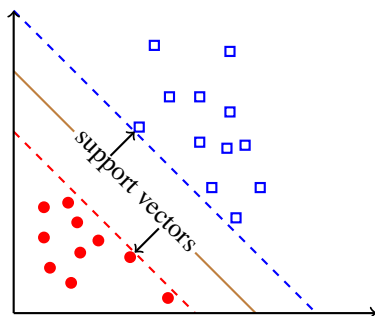


Figure 3: SVM separating hyperplane (Stamp, 2017).

An SVM can also yield a non-linear decision boundary by using the so-called kernel trick (Stamp, 2017). This technique projects input features into a higher-dimensional “feature space” where the data is more

likely to be linearly separable. An example illustrating the effect of the kernel trick is given in Figure 4, where the input space data (left-hand side) is not linearly separable, but after mapping to a higher dimension (right-hand side), we can easily separate the data with a hyperplane. The real “trick” to the kernel trick is that we pay almost no computational penalty for working in this higher dimensional space. A variety of non-linear kernel functions are commonly used. For a given problem, the SVM kernel and its associated parameters are generally selected by experimentation (Polamuri, 2017).

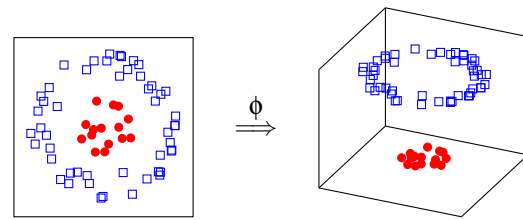


Figure 4: The kernel trick (Stamp, 2017).

2.4.2 Principal Component Analysis

Principal component analysis (PCA) is a linear algebraic technique that provides a powerful tool for dimensionality reduction. Here, we provide a very brief introduction to the topic; for more details, Shlens’ tutorial is highly recommended (Shlens, 2005).

Geometrically, PCA aligns a basis with the (orthogonal) directions having the largest variances. These directions are defined to be the principal components. A simple illustration of such a change of basis appears in Figure 5.

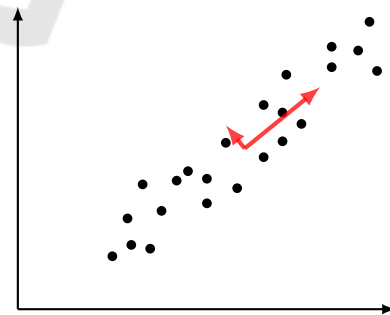


Figure 5: A better basis.

Intuitively, larger variances correspond to more informative data—if the variance is small, the training data is clumped tightly around the mean and we have limited ability to distinguish between samples. In contrast, if the variance is large, there is a much better chance of separating the samples based on the characteristic (or characteristics) under consideration. Con-

sequently, once we have aligned the basis with the variances, we can ignore those directions that correspond to small variances without losing significant information. In fact, small variances often contribute only noise, in which cases we can actually improve our results by neglecting those directions that correspond to small variances. We can often achieve a dramatic dimensionality reduction using PCA.

2.5 Data Collection and Feature Extraction

An accelerometer is a type of sensor that can capture data related to phone movement, and is present in all modern smartphones. The measurements provided by an accelerometer are in terms of acceleration relative to a freefall along the x , y and z axes. The unit of measurement is in terms of gravitational acceleration, which on earth is given by $g = 9.8m/second^2$. For example, if the smartphone is placed flat on the ground, the accelerometer will read 0 along the x and y axis and 1 along the z axis (Fitbit, Inc, 2019).

When the device is moved, the acceleration along the three axes is measured as a sequence of tri-axial data points that can be represented as

$$(x_t, y_t, z_t)$$

where x , y , and z represents the acceleration along these axes and t denotes the time. Smartphone accelerometers allow the sampling time to be user defined. In our research, we fix the sampling rate at 50ms, which means that we obtain 20 triples per second. Thus, in our experiments, if a gesture lasts for 2 seconds, the accelerometer records 40 data points represented as

$$((x_0, y_0, z_0), (x_1, y_1, z_1), (x_2, y_2, z_2), \dots, (x_{39}, y_{39}, z_{39})).$$

We measure a user’s signature, which is of the form

$$sig = ((x_{t_0}, y_{t_0}, z_{t_0}), (x_{t_1}, y_{t_1}, z_{t_1}), \dots, (x_{t_L}, y_{t_L}, z_{t_L})) \quad (1)$$

A signature that requires x seconds to draw results in a length parameter in (1) of $L = \lfloor 40x \rfloor - 1$.

We can connect the datapoints of a signature of the form (1) to yield an object in 3-dimensional space that provides a representation of the signature. For example, Figure 6 shows the result of such a reconstruction when the letter “S” was drawn in the air—for an appropriate rotation, we can clearly see a crude representation of this letter.

2.6 Data Collection

We perform data collection on both Android and Apple iOS platforms. This was done to enabled us to

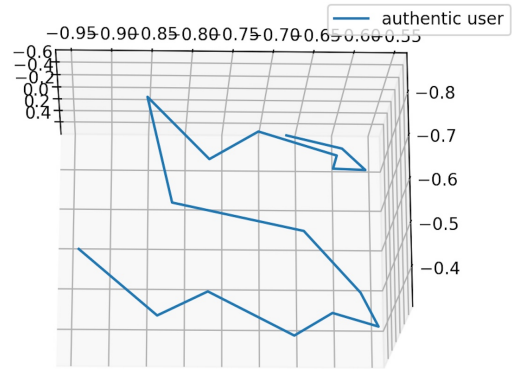


Figure 6: Reconstructed “S” from accelerometer data.

maximize the number of users in our research. For the Android platform, we created a custom application that automatically uploads data to a cloud-based database, Google Firebase (Google, 2019).

A sample of data collected on an Android phone is shown in Figure 7. The data is stored in JSON format. Here, the timestamp at which the signature collection started forms the root of the JSON tree and every tri-axial data point (recorded at 50ms intervals) form the children of this tree.

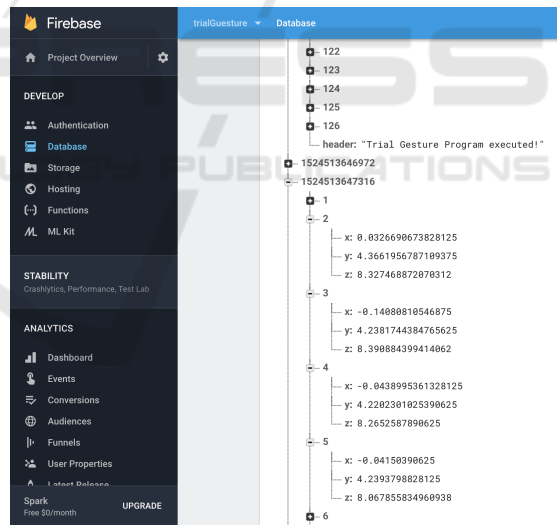


Figure 7: Screenshot of collected data from Android phone.

For the iOS platform, the appropriately-named application Accelerometer was used (DreamArc, 2019). A screenshot of this application is shown in Figure 8. Note that in this case, the signature data is plotted as a curve, based on the time series. Here, acceleration along each axis is represented as a separate curve—the x -axis data is the green curve, y -axis is the red curve, and the z -axis acceleration is the blue curve. Data equivalent to that collected from Android devices is easily derived from these curves.



Figure 8: Data collection in iOS.

Regardless of the platform, the user performs the following steps.

- Click the “start measuring” button on the app, which begins the recording of accelerometer data.
- Move the smartphone in the air to draw a signature.
- Click the “stop measuring” button.

These steps serve to record the data and load it into our database in the cloud. Again, this data is stored in JSON format, as illustrated in Figure 7.

We have collected data from $N = 80$ users—we denote these users as

$$user_0, user_1, \dots, user_{79}.$$

We consider two types of signatures, namely, an “unrestricted” signature and a “common” signature, as described below. We treat $user_0$ as a special case—this user selects a specific signature and generates 20 samples of this signature, which serve as the common signature.

Consider $user_i$, where $i > 0$. As with $user_0$, this user selects a signature and generates 20 samples of the selected signature. We refer to this user-selected signature as this user’s unrestricted signature. Next, $user_i$ observes the signature of $user_0$ and attempts to mimic this signature. Since this “signature” will be common to all users, we refer to this as the common signature. As with the unrestricted signature, we again collect data for 20 iterations of the common signature from each user. This common signature can be used, for example, to analyze the effectiveness of shoulder surfing attacks.

In our experiments, users typically selected their unrestricted signature to be their initials. Data collection generally required about 2 seconds of accelerometer recording time per signature and the entire collection process required about 15 minutes per user.

To summarize, we collect 20 samples of one specific signature from $user_0$, which we denote as the common signature. Then for each $user_i$, where $i > 0$, we collect the following data.

Unrestricted Signature. This is a pattern chosen by the user, and it serves as a signature for the user. This same signature is repeated 20 times and thus we have 20 samples of each user’s unrestricted signature.

Common Signature. The user observes the signature of $user_0$ and attempts to accurately “forge” this signature. This is repeated 20 times, so that we have 20 samples of the common signature from each user.

Our dataset is freely available for use by other researchers (Sundaravaradhan, 2019). The results presented in Section 3 are intended to serve as an initial benchmark for future research involving this dataset.

2.6.1 Feature Extraction

The raw accelerometer data points will serve as features in some of our experiments. In addition, we extract the following derived features from every signature, including both the unrestricted and the common signatures.

Mean. The mean values of the data for each of the three axes is calculated. This gives us three mean values, which we denote as $\mu = (\mu_x, \mu_y, \mu_z)$, where the subscript denotes the coordinate.

Median. The median values of the data for each of the three axes is calculated. We denote the medians in the x , y , and z coordinates as $m = (m_x, m_y, m_z)$.

Magnitude. The magnitude of a signature is defined as the average of the root mean square of the tri-

axial data (Bishal Singha et al., 2017). The magnitude M is calculated as

$$M = \left(\sum_{k=1}^L \sqrt{x_k^2 + y_k^2 + z_k^2} \right) / L$$

where L is the length of the signature.

Velocity. The velocity v is calculated as a vector consisting of the differences in consecutive data points along each of the three axes. The velocity vector is computed as

$$v = \left((v_{x,0}, v_{y,0}, v_{z,0}), (v_{x,1}, v_{y,1}, v_{z,1}), \dots, (v_{x,L-1}, v_{y,L-1}, v_{z,L-1}) \right)$$

where, using the notation in (1), we have

$$v_{x,i} = x_i - x_{i-1}, v_{y,i} = y_i - y_{i-1}, v_{z,i} = z_i - z_{i-1}.$$

3 EXPERIMENTS AND RESULTS

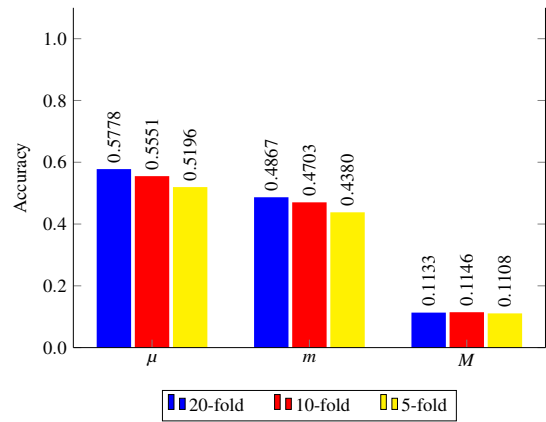
We present the results from three classes of experiments. For our first class of experiments, we consider the problem of distinguishing users, based on their unrestricted signatures, that is, we consider the multiclass classification problem. This experiment can be viewed as representing an identification problem, where we must select the user from among a set of possible users—in the most challenging case, we must distinguish between all users. This is an inherently difficult multiclass problem that will enable us to compare the effectiveness of various machine learning techniques under the most challenging circumstances. For the second class of experiments, we attempt to distinguish a specific user in a one-versus-all mode. This experiment represents a more realistic authentication mode, where we either authenticate a specified user, or not. As our final class of experiments, we consider the common signature data. This case can be viewed as simulating a shoulder surfing attack, where an attacker attempts to mimic a specific signature that they have observed.

For each of these classes of experiments, we test various features and machine learning techniques. Specifically, the machine learning techniques considered are those discussed in Section 2.4, namely, SVMs and PCA.

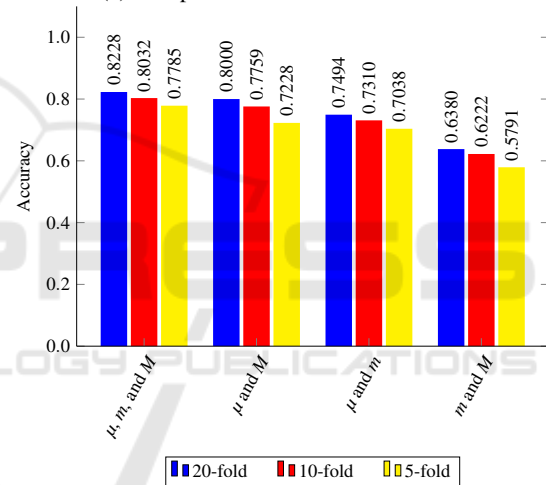
3.1 SVM Experiments

We performed preliminary experiments with various kernels and values of the parameters. We found that the best results were obtained using a Gaussian radial basis function (RBF) kernel. For the hyperparameters, we found that the combination of $\gamma = 0.003$

and $C = 100.0$ yielded the best results. Hence, for all experiments reported in this section, we use an RBF kernel with $\gamma = 0.003$ and $C = 100.0$.



(a) Comparison of features and folds

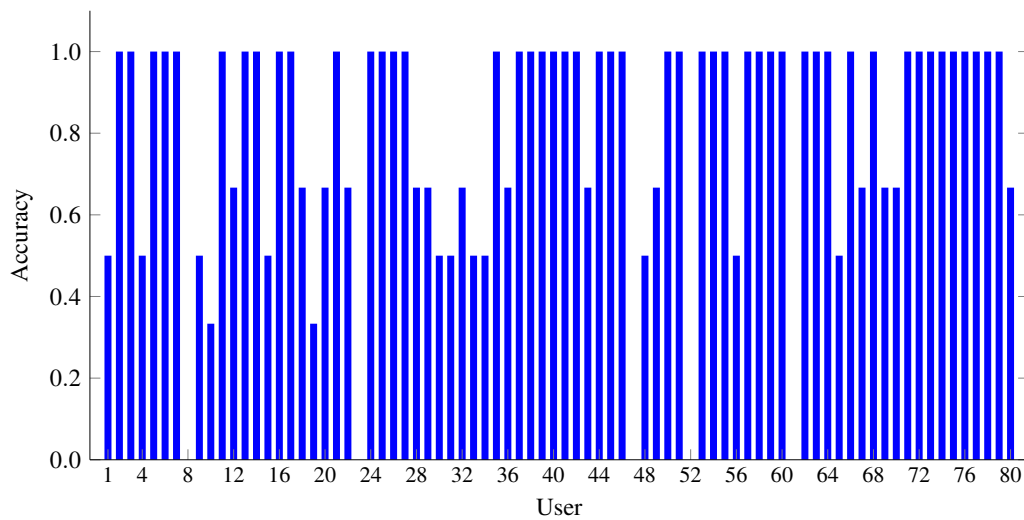


(b) Combinations of features and folds

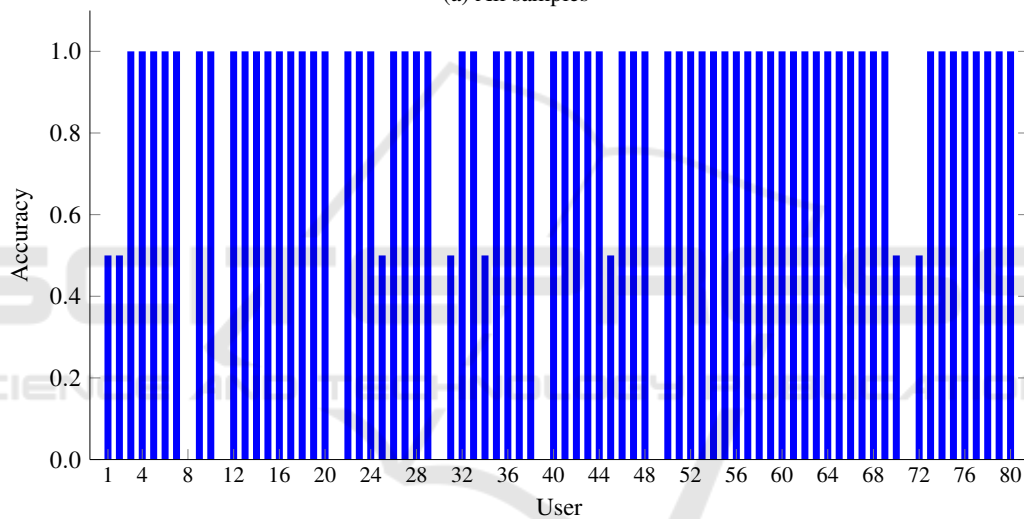
Figure 9: SVM results.

First, we consider the problem of distinguishing a particular users' signature from all other users. In this case, we experiment with each of the three individual features, mean, median, and magnitude, and all combinations of two of these features, as well as all three features. In each case, we perform k -fold cross-validation for $k = 5$, $k = 10$, and $k = 20$. The accuracy results for these experiments are summarized in Figure 9 (a). From the results in Figure 9 (a), we see that the mean is the strongest of the three features considered, and the magnitude is weakest, and we note that none of the individual features performs particularly well.

Next, we consider all combinations of these three features and, again, we experiment with different numbers of folds. These results are summarized in



(a) All samples



(b) Omit last 3 samples

Figure 10: Individual users (all samples with 0.95 training ratio).

Figure 9 (b). We see that although the magnitude M is very weak as a feature by itself, it does contribute useful information when used in combination with other features. The combination of all three features yields the strongest result, with an overall accuracy of more than 82% in the best case.

In Figure 10, we give results for each individual user. Specifically, in these experiments, we attempt to distinguish each user’s signature from all other users, based on the combination of all three features considered above, namely, the mean μ , the median m , and the magnitude M . Note that we obtain an ideal accuracy of 1.0 for 48 of the 80 users.

The ability to distinguish between users signatures is an essential aspect of authentication. The results in Figure 10 (a) indicate that the FRR or insult rate is

sufficiently low so that the this signature data could form the basis for a viable authentication scheme.

During the data collection process, it was observed that users tended to take less care in the last few signatures. Hence, we repeat the individual user experiment summarized in Figure 10 (a), but omitting the last three signatures for each user. The results of these experiments appear in Figure 10 (b). Comparing Figures 10 (a) and 10 (b), we see that in the latter case, the number of users with ideal separation is 62, which is an increase of 14 over the former case. This result suggest that “user fatigue” did indeed set in during data collection, with users taking less care with their last few signatures. Omitting more than the last 3 signatures did not improve on these results, which indicates that only the last few signatures are suspect.

3.2 PCA-SVM Experiments

As another set of experiments, we first project the 3-d accelerometer vectors into two dimensions, based on the two dominant eigenvectors obtained via PCA. The idea here is to convert a 3-d “image”, such as that in Figure 6, into a flat 2-dimensional image. By using PCA to do the flattening, the flattened image may have the characteristics of a letter drawn on a flat surface, effectively removing the third dimension with no loss of information. Intuitively, this should serve to make classification somewhat easier, as we have largely removed noise (specifically, the rotation in 3-d space) from the problem.

Once we have converted all samples to 2-dimensional flat “images”, we use an SVM for classification. For the SVMs, we use a 20-80 test-validation split. We refer to these as PCA-SVM experiments.

For the one-to-all experiments, we obtain a precision of 0.8725 and a recall of 0.8792, which gives us an F1 score of 0.8758. For the multiclass identification problem we must distinguish between multiple users’ signatures. We consider each of the cases where the number of users varies over the range of $n = 2, 3, 4, \dots, 80$. These results are summarized in Figure 11. Note that the $n = 2$ case can be viewed as representative of the authentication problem.

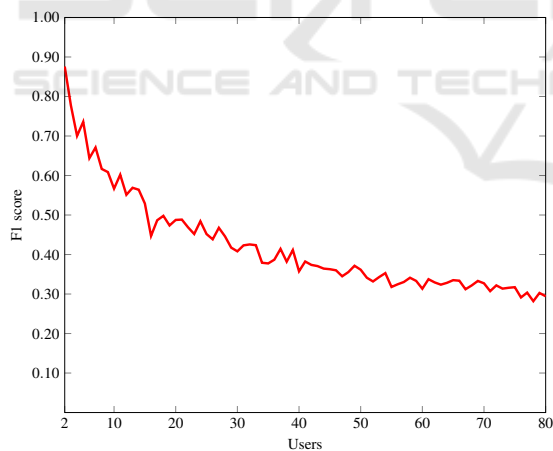


Figure 11: F1 scores for PCA-SVM experiments.

The results in Figure 11 indicate that this PCA-SVM technique is not be particularly strong in an identification mode, where we must distinguish between a large number of users. This is not surprising, given the inherent difficult of the problem, and the fact that our technique is relatively crude, while the data itself is a very brief signature (i.e., only initials). However, the F1-score is nearly 90% for the $n = 2$ case, which indicates that this technique has considerable potential as an authentication mode.

4 CONCLUSION AND FUTURE WORK

In this paper, we introduced a new dataset consisting of biometric accelerometer data collected from 80 subjects. We performed a preliminary analysis of the data using SVMs and PCA. These results indicate that such accelerometer data has potential for use as a practical, lightweight authentication system. Our results also lay the groundwork for future research involving this dataset.

For future work, additional feature engineering will surely be important. Here, we only considered the raw accelerometer data and the most elementary derived features. With respect to machine learning and deep learning techniques, we believe that convolutional neural networks (CNN) would be a viable approach to the problem—the accelerometer data has a natural interpretation in terms of a 3-d image, and previous work has employed CNNs to authenticate users based on sensor data (Singh et al., 2017).

REFERENCES

- Alariki, A. A. and Manaf, A. A. (2014). Touch gesture authentication framework for touch screen mobile devices. *Journal of Theoretical and Applied Information Technology*, 62(2):493–498.
- Anderson, R. J. (2001). *Security Engineering: A Guide to Building Dependable Distributed Systems*. John Wiley & Sons, Inc., New York, NY, USA, 1st edition.
- Bailador, G., Sanchez-Avila, C., Guerra-Casanova, J., and de Santos Sierra, A. (2011). Analysis of pattern recognition techniques for in-air signature biometrics. *Pattern Recognition*, 44(10):2468 – 2478. Semi-Supervised Learning for Visual Content Analysis and Understanding.
- Bishal Singha, T., Nath, R. K., and Narsimhadhan, A. V. (2017). Person recognition using smartphones’ accelerometer data. <https://arxiv.org/abs/1711.04689>.
- Bradley, A. P. (1997). The use of the area under the ROC curve in the evaluation of machine learning algorithms. *Pattern Recognition*, 30(7):1145–1159.
- Clark, G. D. and Lindqvist, J. (2014). Engineering gesture-based authentication systems. <https://arxiv.org/pdf/1408.6010.pdf>.
- DreamArc (2019). Accelerometer. <https://itunes.apple.com/us/app/accelerometer/id499629589>.
- Fitbit, Inc (2019). Accelerometer Sensor Guide. <https://dev.fitbit.com/build/guides/sensors/accelerometer>.
- Ganesh, S. M., Vijayakumar, P., and Deborah, L. J. (2017). A Secure Gesture Based Authentication Scheme to

- Unlock the Smartphones. In *2017 Second International Conference on Recent Trends and Challenges in Computational Models (ICRTCCM)*, pages 153–158.
- Google (2019). Firebase. <https://firebase.google.com>.
- Guse, D. (2011a). Gesture-based User Authentication on Mobile Devices using Accelerometer and Gyroscope. Master's thesis, Berlin Institute of Technology.
- Guse, D. (2011b). Gesture-based user authentication on mobile devices using accelerometer and gyroscope. Master thesis, Technische Universität Berlin.
- Huang, C., Yang, Z., Chen, H., and Zhang, Q. (2017). Signing in the Air w/o Constraints: Robust Gesture-Based Authentication for Wrist Wearables. In *GLOBECOM 2017 - 2017 IEEE Global Communications Conference*, pages 1–6.
- Huang, J., Troia, F. D., and Stamp, M. (2018). Acoustic gait analysis using support vector machines. In *4th International Conference on Information Systems Security and Privacy, ICISSP 2018*, pages 545–552.
- Imura, S. and Hosobe, H. (2018). A hand gesture-based method for biometric authentication. <http://www.hosobe.org/wp-content/uploads/hcii2018.pdf>.
- Liu, C., Clark, G. D., and Lindqvist, J. (2017). Guessing Attacks on User-Generated Gesture Passwords. *Proc. ACM Interact. Mob. Wearable Ubiquitous Technol.*, 1(1):3:1–3:24.
- Liu, J., Zhong, L., Wickramasuriya, J., and Vasudevan, V. (2009a). uWave: Accelerometer-based personalized gesture recognition and its applications. *Pervasive and Mobile Computing*, 5(6):657 – 675. PerCom 2009.
- Liu, J., Zhong, L., Wickramasuriya, J., and Vasudevan, V. (2009b). uWave: Accelerometer-based personalized gesture recognition and its applications. *Pervasive and Mobile Computing*, 5:657–675.
- Lu, D., Xu, K., and Huang, D. (2018). A data driven in-air-handwriting biometric authentication system. In *IEEE International Joint Conference on Biometrics, IJCB 2017*, pages 531–537.
- Meng, Y., Wong, D. S., Schlegel, R., and Kwok, L.-f. (2013). Touch gestures based biometric authentication scheme for touchscreen mobile phones. In Kutylowski, M. and Yung, M., editors, *Information Security and Cryptology*, pages 331–350.
- Mitra, S. and Acharya, T. (2007). Gesture Recognition: A Survey. *IEEE Transactions on Systems, Man, and Cybernetics, Part C (Applications and Reviews)*, 37(3):311–324.
- Palamuri, S. (2017). SVM classifier implementation in Python with scikit-learn. <http://dataaspirant.com/2017/01/25/svm-classifier-implementation-python-scikit-learn/>.
- Rabiner, L. R. (1989). A tutorial on hidden Markov models and selected applications in speech recognition. *Proceedings of the IEEE*, 77(2):257–286.
- Shlens, J. (2005). A tutorial on principal component analysis. <http://www.cs.cmu.edu/~elaw/papers/pca.pdf>.
- Singh, M. S., Pondenkandath, V., Zhou, B., Lukowicz, P., and Liwickit, M. (2017). Transforming sensor data to the image domain for deep learning - An application to footstep detection. In *2017 International Joint Conference on Neural Networks (IJCNN)*, pages 2665–2672.
- Stamp, M. (2011). *Information Security: Principles and Practice*. Wiley, 2nd edition.
- Stamp, M. (2017). *Introduction to Machine Learning with Applications in Information Security*. Chapman and Hall/CRC, Boca Raton.
- Sundaravaradhan, P. (2019). Gesture dataset. [gestureData.zip](https://github.com/sundaravaradhan/gestureData).
- Suriya Prakash, J., Annamalai Vignesh, K., Ashok, C., and Adithyan, R. (2012). Multi class support vector machines classifier for machine vision application. In *2012 International Conference on Machine Vision and Image Processing, MVIP 2012*, pages 197–199.
- Yang, J., Li, Y., and Xie, M. (2015). MotionAuth: Motion-based authentication for wrist worn smart devices. In *2015 IEEE International Conference on Pervasive Computing and Communication Workshops (PerCom Workshops)*, pages 550–555.
- Yang, L., Guo, Y., Ding, X., Han, J., Liu, Y., Wang, C., and Hu, C. (2015). Unlocking Smart Phone through Handwaving Biometrics. *IEEE Transactions on Mobile Computing*, 14(5):1044–1055.